12. AN EVALUATION OF TRANSONIC SPILLAGE DRAG BASED ON

TEST RESULTS FROM LARGE-SCALE INLET MODELS

By Warren E. Anderson, Martine W. Petersen[1],
and Norman E. Sorensen
NASA Ames Research Center

SUMMARY

Transonic spillage drag is evaluated on the basis of test results of three experimental inlet research programs. The additive-drag component of spillage drag was calculated from experimental measurements on both axisymmetric and two-dimensional type inlet models. In both cases, the theoretical prediction of additive drag required a precise knowledge of the pressure distribution on the compression surface.

Cowl lip suction force, which acts to cancel a portion of the additive drag, was measured on a two-dimensional spillage-drag model. The effects of a wide variety of geometric factors were studied on this model. It was found, for example, that a significant cancellation (large cowl lip suction force) occurred subsonically for a wide range of cowl lip shapes, whereas the effect at higher supersonic Mach numbers was small.

INTRODUCTION

In recent years the development of high-performance aircraft has focused attention on the propulsion penalties associated with inlet-engine matching requirements. During off-design operation, one penalty of major importance is inlet spillage drag, particularly in the transonic Mach number range where effects on vehicle performance can be large.

Recently, three experimental inlet research programs have been in progress at the Ames Research Center. Two of the programs involve large-scale axisymmetric and two-dimensional models being tested in support of the supersonic transport. These models have provided data for the two spillage-drag components, additive drag and cowl lip suction force. A third program was an Air Force supported contractual study of spillage drag in two-dimensional inlets. This study involved investigation of a wide variety of inlet geometries and directed considerable attention to both additive drag and lip forces on the cowl and side wall.

This paper will present representative test results from all three models within the Mach number range from 0.6 to 1.3. Some comparisons with available theoretical predictions are also included.

---

[1]Propulsion and Thermo Analysis Engineering Specialist - North American Aviation, Inc., Los Angeles Division

SYMBOLS

A	area
C_D	drag coefficient, $\dfrac{\text{drag}}{qA}$
D_a	additive drag
D_{c_0}	reference cowl drag
ΔD_c	cowl suction force
D_c	cowl drag
D_{cs}	compression surface drag
D_E	inlet system external drag
$D_{SPILLAGE}$	$D_a - \Delta D_c$
K_{ADD}	incremental additive-drag correction factor, $\dfrac{\Delta D_{SPILLAGE}}{\Delta D_a}$
m_i	inlet mass flow
$\dfrac{m_i}{m_\infty}$	inlet mass-flow ratio
M_∞	free-stream Mach number
P	static pressure
P_{t_∞}	free-stream total pressure
$\bar{P}_{t_2}$	area weighted average total pressure at engine-face station
q	dynamic pressure
V	velocity
δ	angle, deg

Subscripts

c	capture
i	inlet
o	initial conditions in stream tube

REF   reference

X   station

∞ free stream

DISCUSSION

The concepts basic to an understanding of the spillage drag are discussed in many publications (e.g., refs. 1 through 5). The following paragraphs, therefore, cover the basic descriptions and definitions only in rather broad and simplified terms.

Inlet system drag definitions are presented in figure 1 together with an illustration showing the effect of inlet mass-flow ratio on the drag components. The term D_{c_O} is the cowl drag at a reference mass-flow ratio (operating condition) and includes the external-cowl pressure and friction drag chargeable to the propulsion system. The variation of cowl pressure drag with mass-flow ratio, ΔD_c, is negative and is referred to as the cowl lip suction force. The spillage drag by definition is equal to $D_a - \Delta D_c$.

Additive drag, D_a, is a force correction which is applied in equating internal thrust and external drag for purposes of evaluating vehicle performance; it is a bookkeeping item for making the definition of thrust and drag compatible and is not a force felt on the vehicle surface. However, it represents a performance factor which the propulsion aerodynamicist can control. The influence of additive drag on mission performance is analyzed in reference 1.

The general expression for additive drag is developed in figure 2 with the aid of a simplified sketch of an inlet flow field. The net force on the entering stream tube element, indicated by the dashed lines, is equal to the momentum change within the element. A summation of forces and rearrangement of terms yields an equation which states that the additive drag is equal to the momentum change plus the inlet pressure force plus the compression surface drag. Finally, the additive drag coefficient is referenced to the inlet capture area, A_c, as shown. The equation for additive drag differs for different inlet geometries; an open nose inlet requires only the first two terms or total-momentum change, whereas a two-dimensional inlet with side walls requires a fourth term similar to that for the ramp compression surface, to account for the side-wall pressure and friction drag.

EXPERIMENTAL RESULTS

Additive-Drag Measurements

Transonic additive-drag measurements were made on two large-scale inlet models. One of the models was axisymmetric with a capture diameter of 20.0 inches. The other inlet model was two-dimensional with a capture height and width of 14.0 inches. Both models are described in reference 6.

Additive-drag values were obtained from a momentum balance as shown in figure 2. In the axisymmetric inlet, total and static-pressure rakes were installed on the centerbody at the maximum diameter station. These rakes were used to measure the inlet total-momentum change and inlet mass-flow ratio. The centerbody was instrumented with static-pressure orifices (area weighted) from which the centerbody pressure drag was computed. Figure 3 shows typical additive-drag values and the corresponding total-pressure recovery at the engine face for several Mach numbers and a range of inlet mass-flow ratios. For these tests, the centerbody was a 12.5° half-angle cone and the cowl lip was positioned at the maximum diameter. Near the maximum mass-flow ratio, inlet choking caused a large reduction in pressure recovery and little decrease in additive drag. Reducing mass-flow ratio produced the characteristic increase in additive drag at all Mach numbers. Data obtained with the cowl lip at more forward positions indicated similar families of curves, but with higher values of additive drag and total-pressure recovery.

Figure 4 shows the minimum additive-drag coefficients measured for three centerbody shapes at transonic Mach numbers. The lower curve is for the 12.5° half-angle cone. The two upper curves are for isentropic surfaces that had initial cone angles of 5° and 10° and curved to a total compression of 15°. The minimum additive drag has a peak at $M_\infty = 1.1$ for all three centerbody shapes. A computer program employing the method of characteristics was used to calculate the supersonic additive-drag curve for the 12.5° cone. Although an extrapolation of this curve to transonic Mach numbers would fair into the peak measured value of minimum additive drag for the 12.5° cone, the drag at low supersonic Mach numbers is overestimated. The experimental results show that the total-momentum change (represented by the first two terms of the additive-drag equation) is nearly zero at high mass-flow ratios and the additive drag is almost equal to the centerbody drag (the filled symbols). Measured static-pressure ratio distributions used to calculate the centerbody drag for Mach numbers 0.8 and 1.0 are presented in figure 5. The pressures are seen to change rapidly near the maximum centerbody diameter; to calculate additive drag theoretically, the theory must be able to predict the pressures in this region to an exact degree.

Figure 6 shows the total-pressure recovery at the engine face and the corresponding values of additive-drag coefficient computed for optimized[2] operating conditions of a supersonic transport engine. These values are compared with the minimum measured values of additive drag and the corresponding total-pressure recoveries. For optimized operating conditions the cowl lip was slightly forward of the maximum centerbody diameter and the additive drag was substantially higher than the minimum values.

In summary, the momentum-balance method appears to be satisfactory for experimentally evaluating the transonic additive drag of axisymmetric type inlets. Nearly all the additive drag at full flow conditions is centerbody pressure drag. For theoretical predictions of additive drag, it is therefore necessary to have accurate knowledge of the centerbody pressure distribution.

---

[2]The optimum inlet-engine operating condition is at the maximum value of net thrust minus additive drag.

The additive drag at the optimized engine-inlet operating conditions is substantially higher than the minimum measured values.

The two-dimensional inlet model was instrumented in a manner similar to the axisymmetric model. Measurements of static pressure at the cowl lip station and of inlet mass-flow ratio permitted calculation of the momentum terms of the additive-drag equation. The ramp and side-wall drag values were obtained from static-pressure measurements on these surfaces. Figure 7 shows the variation of engine-face total-pressure recovery and inlet additive-drag coefficient with inlet mass-flow ratio. Included in the figure is a sketch of the inlet showing the cowl lip located slightly forward of the minimum throat station. Also indicated are other geometric features of the configuration, that is, ramp, sharp cowl lip, and extended side walls. Results are shown for tests with and without boundary-layer bleed on the ramp and side-wall surfaces in the throat region. The bleed increased the total-pressure ratio and the maximum mass-flow ratio considerably at Mach numbers of 1.0 and 1.275. Losses at a Mach number of 1.275 remain relatively high, however, and suggest that substantial friction effects were present. Note that the use of boundary-layer bleed does not change the basic curves of additive-drag coefficient. This should be expected since the bleed surfaces are downstream of the lip station; the data indicate consistency in the additive-drag measurements.

The ability to calculate additive drag theoretically is valuable for inlet design and vehicle performance studies. Figure 8 presents results from theoretical and semiempirical calculations of minimum additive-drag coefficients compared to the experimental values. In this case, the theory is based on the assumption of one-dimensional flow relationships from the free stream to the cowl-lip station and considers theoretical shock losses only. To calculate ramp drag, the ramp pressure was assumed to vary linearly from either free-stream or downstream shock-wave conditions at the ramp leading edge to the inlet conditions at the cowl lip. The basic theoretical curve is in fair agreement with experiment at Mach numbers below 1.0, but agreement is poor at other Mach numbers. However, if experimental ramp and side-wall drag is used in place of that calculated from the assumed linear pressure distribution, agreement is greatly improved. Also, another unrealistic assumption in the basic theory was that only shock losses affect the momentum balance. Figure 7 indicates that the two-dimensional inlet configuration had substantial friction losses at $M_\infty = 1.275$ because of the long perforated ramp and side-wall surfaces forward of the lip station. If these losses are accounted for in the theoretical calculation of conditions at the lip station, the results shown compare reasonably well with those obtained experimentally.

The Ames tests of additive drag on a two-dimensional inlet are summarized as follows. Experimental techniques provide accurate measurements of additive drag. Theoretical predictions of two-dimensional additive drag are excessively high at supersonic Mach numbers unless the ramp drag and total-pressure losses at the inlet lip station are accurately determined.

Spillage-Drag Measurements

Force-balance measurements of spillage drag on large-scale complete inlet models generally provide only qualitative results. It is inherently difficult to obtain accurate values since the basic model drag forces are large relative to the spillage-drag increments of interest. A model was therefore specially designed and constructed for measuring spillage drag accurately. The tests were conducted so as to ensure maximum accuracy of the results. A photograph of the model mounted in the wind tunnel is shown in figure 9. The test program studied a wide variety of geometric factors affecting the spillage drag of rectangular (two-dimensional) supersonic inlets. Several cowls, side walls, and fixed initial ramps could be interchanged on the model. The second ramp was variable from 5° to 12° relative to the free-stream vector. The model and test results are completely described in reference 5.

One feature of this spillage-drag investigation was the determination of external pressure drag for the cowl plus side wall. Only meager information exists on this important component of the total external drag of two-dimensional inlets. The incremental change in external pressure drag when mass flow is reduced from a reference mass-flow ratio[3] is, of course, the lip suction force which was discussed earlier. Six of the cowl shapes which were instrumented for static-pressure measurements are described in figure 10. Cowls 1, 2, and 3 had circular-arc external surfaces, whereas the remaining three were straight external angle cowls. Cowl and side-wall external pressure drag characteristics for cowls 1, 2, 4, and 6 are shown in figure 11 for a range of mass-flow ratios at Mach numbers 0.84 and 1.29. The ramp angle and the side-wall external angle were held fixed for this comparison at 5° and 6°, respectively. In addition, the side-wall leading edge was cut back at an angle coincident with the initial ramp compression shock wave at a free-stream Mach number of 3.0. All of the cowl shapes yield suction forces which would allow partial cancellation of the additive drag at reduced mass-flow conditions. It is interesting that the drag becomes negative and these surfaces actually produce thrust at mass-flow ratios somewhat less than the reference value. At subsonic conditions ($M_\infty = 0.84$) circular-arc cowls 1 and 2 have lowest drag at high mass-flow ratios and straight cowl 6 has the best lip suction capabilities. The curves for Mach number 1.29 indicate that low angle cowls 1 and 4 provide the best performance. At higher supersonic speeds, cowl 4 with the lowest cowl angle provided the best drag characteristics.

Force-balance measurements of total external drag were obtained for various geometric configurations of the spillage-drag model. The incremental change in external drag as the mass-flow ratio is reduced below the reference value is, in effect, the increment in spillage drag (see fig. 1). (This change differs from the incremental change in additive drag by the amount of the lip suction force.) The increment in spillage drag, measured by a force balance, divided by the corresponding change in additive drag is defined as K_{ADD}, the incremental additive-drag correction factor. The amount of additive drag change which appears as a change in spillage drag is indicated by K_{ADD} as follows.

---

[3]Reference mass-flow ratio is defined in this case as a value equal to the inlet area, A_i, divided by the capture area, A_c.

$$D_{SPILLAGE} = \Delta D_{SPILLAGE} + D_{a_{REF}}$$

$$D_{SPILLAGE} = K_{ADD}\Delta D_a + D_{a_{REF}}$$

Figure 12 presents curves of K_{ADD} based on theoretically computed values of ΔD_a as a function of mass-flow ratio for cowls 4 and 6 (agreement between measured and theoretically computed ΔD_a was good for all cowls tested). The figure shows additive-drag corrections at $M_\infty = 0.84$ are greater (numerically lower), and are affected less by mass-flow ratio than those at $M_\infty = 1.29$. Also, these corrections are affected more by Mach number than by the cowl lip shape.

In addition to the results presented, the tests of the spillage-drag model provided the following information.

1. Lower spillage drag was obtained by rotating the external ramp of the inlet, to deflect excess airflow, than by rotating the cowl. However, the combined rotation of both cowl and ramp would provide the lowest spillage drag.

2. Blunting the leading edge of a 10° circular-arc cowl with 0.040-inch and 0.100-inch radii had little effect upon additive-drag cancellation but increased total external drag chargeable to the inlet.

3. Ramp pressure drags and cowl plus side-wall external drag measured for a number of configurations are useful in determining total inlet drag penalties.

4. Mathematical models for computation of theoretical additive drag, that were devised and programmed for computer usage, were confirmed by the test results.

REFERENCES

1. Mount, Joseph S.: The Effect of Additive Drag Upon Aircraft Performance. Paper No. 64-599, Am. Inst. Aeron. Astronaut., Aug. 1964.

2. Davis, Wallace F.; and Scherrer, Richard: Aerodynamic Principles for the Design of Jet-Engine Induction Systems. NACA RM A55F16, 1956.

3. Sibulkin, Merwin: Theoretical and Experimental Investigation of Additive Drag. NACA Rept. 1187, 1954. (Supersedes NACA RM E51B13.)

4. Davis, Wallace F.; and Gowen, Forrest E.: The Change With Mass-Flow Ratio of the Cowl Pressure Drag of Normal-Shock Inlets at Supersonic Speeds. NACA RM A56C06, 1956.

5. Petersen, Martine W., and Tamplin, Gordon C.: Experimental Review of
    Transonic Spillage Drag of Rectangular Inlets. AFAPL-TR-66-30,
    U.S. Air Force, May 1966.

6. Sorensen, Norman E., Anderson, Warren E., Wong, Norman D., and
    Smeltzer, Donald B.: Performance Summary of a Two-Dimensional and an
    Axisymmetric Supersonic-Inlet System. Paper No. 11, NASA Conference
    on Aircraft Aerodynamics, May 1966.

INLET SYSTEM DRAG DEFINITIONS

INLET MASS-FLOW RATIO, m_i/m_∞
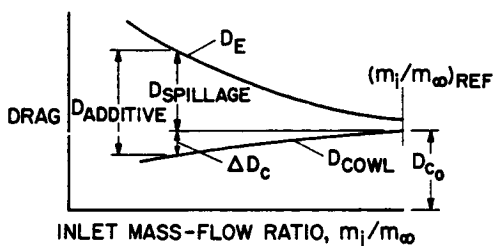
THE EXTERNAL DRAG OF AN INLET SYSTEM IS D_E

$$D_E = D_{COWL} + D_{ADDITIVE} = D_c + D_a$$

$$D_c = D_{c_0} - \Delta D_c$$

$$D_E = D_{c_0} - \Delta D_c + D_a$$

$$D_{SPILLAGE} = D_a - \Delta D_c$$

Figure 1

ADDITIVE DRAG
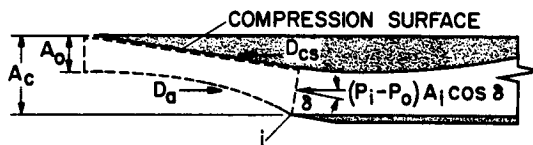
CONSIDERING THE ENTERING STREAM TUBE ELEMENT

NET FORCE = MOMENTUM CHANGE

$$D_a - (P_i - P_0) A_i \cos \delta - D_{cs} = m_i (V_i \cos \delta - V_0)$$

TOTAL MOMENTUM

$$D_a = m_i (V_i \cos \delta - V_0) + (P_i - P_0) A_i \cos \delta + D_{cs}$$

$$C_{D_a} = \frac{D_a}{q_0 A_c}$$

Figure 2

179

AXISYMMETRIC INLET PERFORMANCE
12.5° CONE

ENG-FACE PRESSURE RECOVERY, $\dfrac{\bar{P}_{t_2}}{P_{t_\infty}}$

ADDITIVE DRAG COEFFICIENT, C_{D_a}

INLET MASS-FLOW RATIO, m_l/m_∞

M_∞
- ○ 0.6
- □ .8
- △ 1.0
- ◇ 1.1
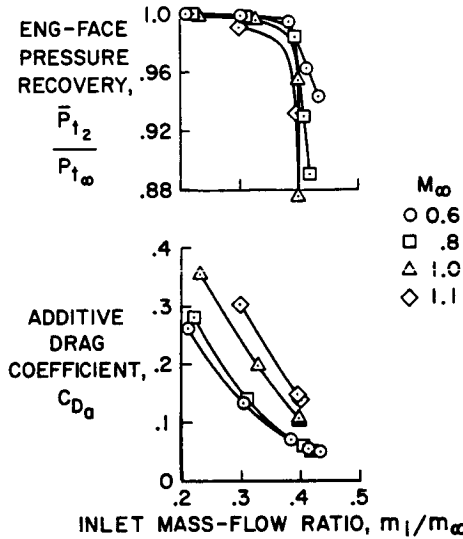
Figure 3

AXISYMMETRIC INLET
MINIMUM ADDITIVE DRAG

□ 5° △ 10° ○ 12.5°

15°

MAXIMUM CENTERBODY DIAMETER

THEORETICAL $12\frac{1}{2}°$ CONE

MINIMUM ADDITIVE DRAG COEFFICIENT, $C_{D_{a_{MIN}}}$

◆ $C_{D_{CONE}}$

FREE-STREAM MACH NUMBER, M_∞

Figure 4

180
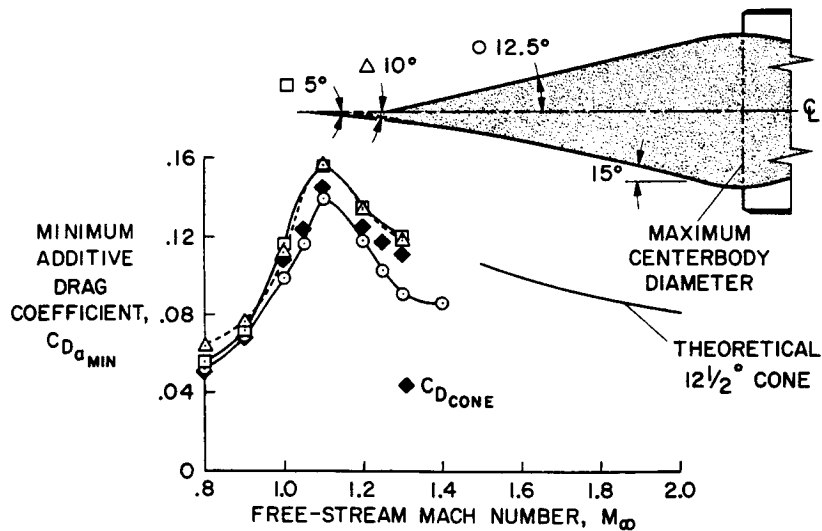
AXISYMMETRIC INLET
TYPICAL CONE STATIC-PRESSURE RATIOS

Figure 5

AXISYMMETRIC INLET
OPTIMIZED ADDITIVE DRAG
$12\frac{1}{2}°$ CONE
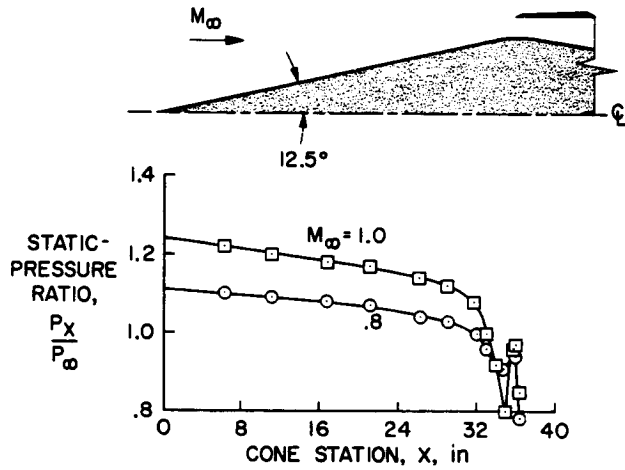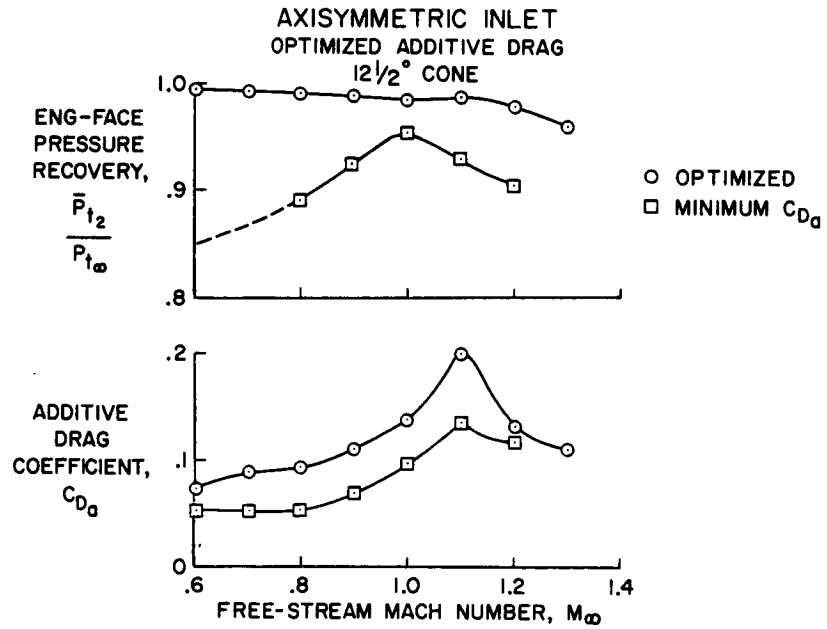
Figure 6

TWO-DIMENSIONAL INLET PERFORMANCE
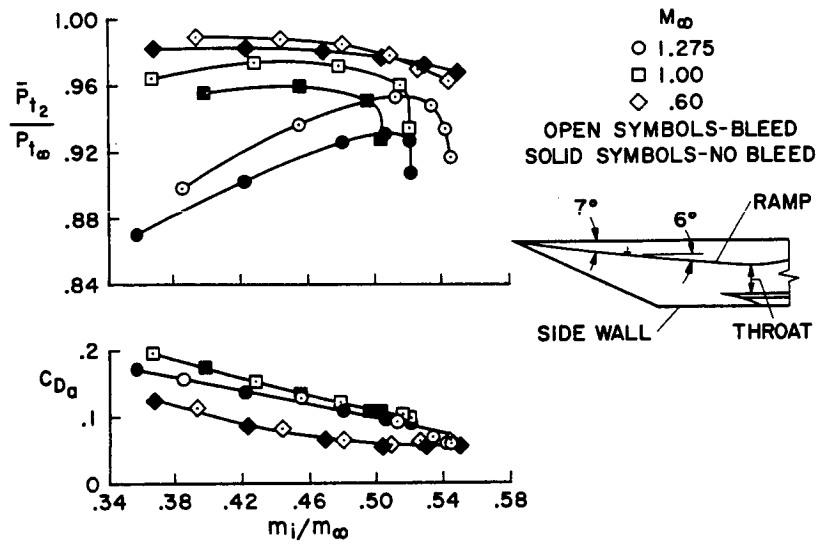
Figure 7

TWO-DIMENSIONAL INLET
THEORETICAL ADDITIVE DRAG
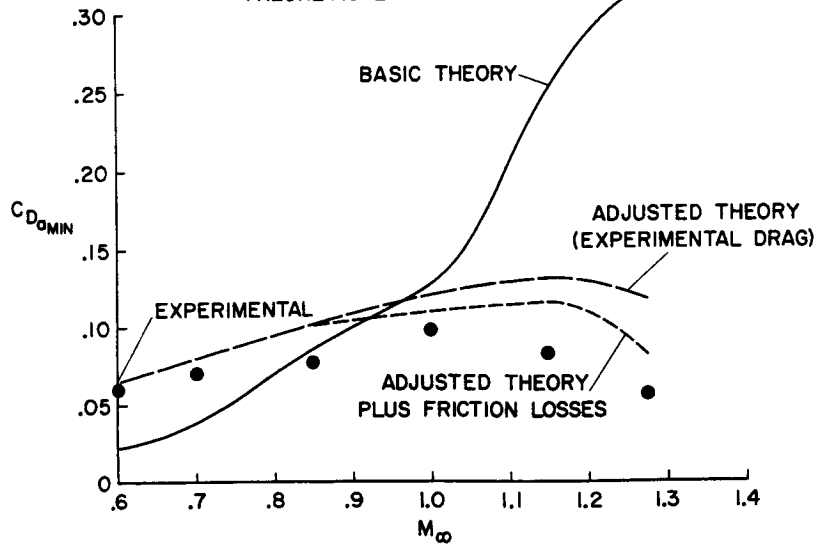
Figure 8

SPILLAGE-DRAG MODEL
INSTALLATION
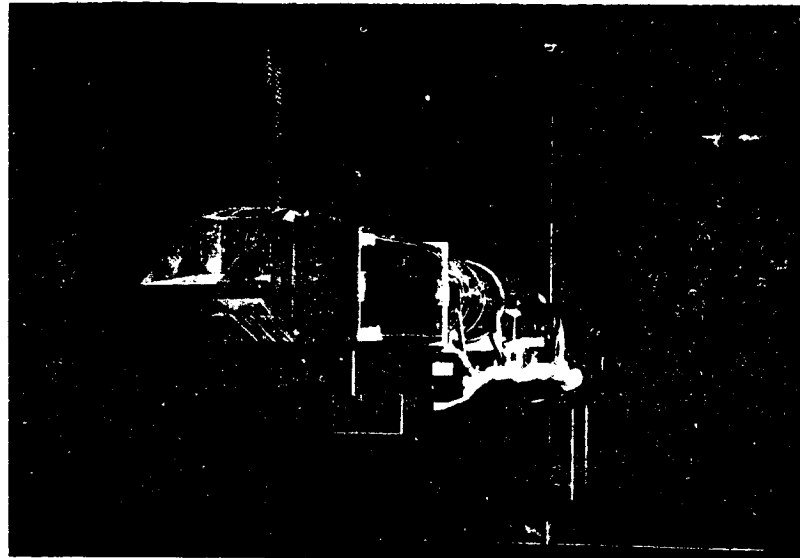
A-35112

Figure 9

SPILLAGE-DRAG MODEL
COWL LIP SHAPES
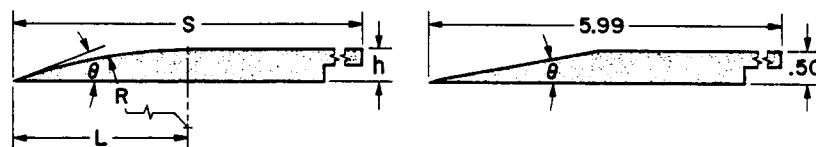
COWL	L	R	θ	S	h
C1	5.71	32.9	10°	5.99	0.50
C2	3.79	14.7	15°	5.99	.50
C3	7.95	29.3	15°	7.99	1.00

COWL	θ
C4	6°
C5	10°
C6	15°

ALL DIMENSIONS IN INCHES

Figure 10

SPILLAGE-DRAG MODEL
COWL PLUS SIDEWALL PRESSURE DRAG

$(m_i/m_\infty)_{REF}$ .796

$M_\infty = .84$

$C_{D_{COWL + S.W.}}$

C1
C2
C4
C6

m_i/m_∞

$(m_i/m_\infty)_{REF}$ .780

$M_\infty = 1.29$

C6
C2
C4
C1

m_i/m_∞
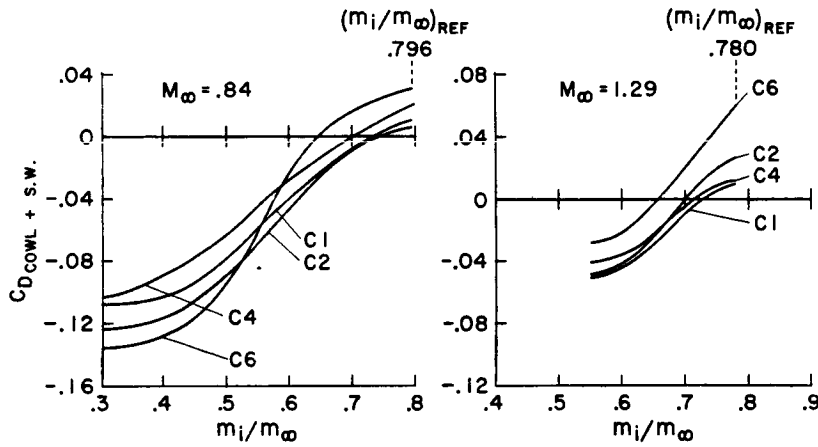
Figure 11

SPILLAGE-DRAG MODEL
INCREMENTAL ADDITIVE DRAG CORRECTION FACTOR

$$K_{ADD} = \frac{\Delta D_{SPILLAGE}}{\Delta D_a}$$

C4

$M_\infty = 1.29$

C6

K_{ADD}

C4

C6

$M_\infty = .84$

m_i/m_∞

Figure 12